# Search for Hidden-Sector Bosons in $B^0 \to K^{*0}\mu^+\mu^-$ Decays

R. Aaij *et al.*[*]
(LHCb Collaboration)

(Received 18 August 2015; published 16 October 2015)

A search is presented for hidden-sector bosons, $\chi$, produced in the decay $B^0 \to K^*(892)^0\chi$, with $K^*(892)^0 \to K^+\pi^-$ and $\chi \to \mu^+\mu^-$. The search is performed using $pp$-collision data corresponding to 3.0 fb$^{-1}$ collected with the LHCb detector. No significant signal is observed in the accessible mass range $214 \le m(\chi) \le 4350$ MeV, and upper limits are placed on the branching fraction product $\mathcal{B}(B^0 \to K^*(892)^0\chi) \times \mathcal{B}(\chi \to \mu^+\mu^-)$ as a function of the mass and lifetime of the $\chi$ boson. These limits are of the order of $10^{-9}$ for $\chi$ lifetimes less than 100 ps over most of the $m(\chi)$ range, and place the most stringent constraints to date on many theories that predict the existence of additional low-mass bosons.

DOI: 10.1103/PhysRevLett.115.161802 PACS numbers: 13.85.Rm, 12.60.-i, 13.20.He, 14.80.Va

Interest has been rekindled in hidden-sector theories [1], motivated by the current lack of evidence for a dark matter particle candidate and by various cosmic-ray anomalies [2–8]. These theories postulate that dark matter particles interact feebly with all known particles, which is why they have escaped detection. Such interactions can be generated in theories where hidden-sector particles are singlet states under the standard model (SM) gauge interactions. Coupling between the SM and hidden-sector particles may then arise via mixing between the hidden-sector field and any SM field with an associated particle that is not charged under the electromagnetic or strong interaction (the Higgs and $Z$ bosons, the photon, and the neutrinos). This mixing could provide a so-called portal through which a hidden-sector particle, $\chi$, may be produced if kinematically allowed.

Many theories predict that TeV-scale dark matter particles interact via GeV-scale bosons [9–11] ($c = 1$ throughout this Letter). Previous searches for such GeV-scale particles have been performed using large data samples from many types of experiments (see Ref. [12] for a summary). These searches have placed stringent constraints on the properties of the hidden-sector photon and neutrino portals; however, the constraints on the axial-vector and scalar portals are significantly weaker.

One class of models involving the scalar portal hypothesizes that such a $\chi$ field was responsible for an inflationary period in the early Universe [13], and may have generated the baryon asymmetry observed today [14,15]. The associated inflaton particle is expected to have a mass in the range $270 \lesssim m(\chi) \lesssim 1800$ MeV [13]. Another class of models invokes the axial-vector portal in theories of dark matter that seek to address the cosmic-ray anomalies, and to explain the suppression of charge-parity ($CP$) violation in strong interactions [16]. These theories postulate an additional fundamental symmetry, the spontaneous breaking of which results in a particle called the axion [17]. To couple the axion portal to a hidden sector containing a TeV-scale dark matter particle, while also explaining the suppression of $CP$ violation in strong interactions, Ref. [18] proposes an axion with $360 \lesssim m(\chi) \lesssim 800$ MeV and an energy scale, $f(\chi)$, at which the symmetry is broken in the range $1 \lesssim f(\chi) \lesssim 3$ TeV. A broader range of $m(\chi)$ and $f(\chi)$ values is allowed in other dark matter scenarios involving axion(-like) states [19–21].

This Letter reports a search for a hidden-sector boson produced in the decay $B^0 \to K^{*0}\chi$, with $\chi \to \mu^+\mu^-$ and $K^{*0} \to K^+\pi^-$ [throughout this Letter, $K^{*0} \equiv K^*(892)^0$ and the inclusion of charge-conjugate processes is implied]. Enhanced sensitivity to hidden-sector bosons arises because the $b \to s$ transition is mediated by a top quark loop at leading order (see Fig. 1). Therefore, a $\chi$ boson with $2m(\mu) < m(\chi) < m(B^0) - m(K^{*0})$ and a sizable top quark coupling, e.g., obtained via mixing with the Higgs sector, could be produced at a substantial rate in such decays. The $B^0 \to K^{*0}\chi$ decay is chosen instead of $B^+ \to K^+\chi$, since better $\chi$ decay time resolution is obtained due to the presence of the $K^+\pi^-$ vertex, and because there is less background contamination. The data used correspond to

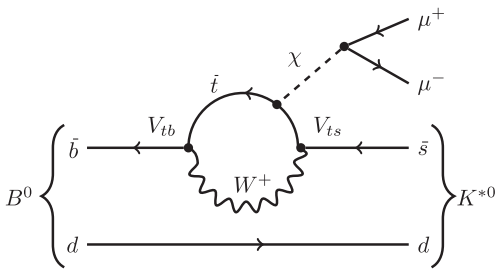


FIG. 1. Feynman diagram for the decay $B^0 \to K^{*0}\chi$, with $\chi \to \mu^+\mu^-$.

[*]Full author list given at the end of the article.



 

integrated luminosities of 1.0 and 2.0 fb$^{-1}$ collected at center-of-mass energies of $\sqrt{s} = 7$ and 8 TeV in $pp$ collisions with the LHCb detector. This is the first dedicated search over a large mass range for a hidden-sector boson in a decay mediated by a $b \to s$ transition at leading order, and the most sensitive search to date over the entire accessible mass range. Previous limits set on $\chi$ boson production in such decays have either focused on a limited mass range [22], or have been obtained from more general searches for long-lived particles [23].

The LHCb detector is a single-arm forward spectrometer covering the pseudorapidity range $2 < \eta < 5$, designed for the study of particles containing $b$ or $c$ quarks [24,25]. The detector includes a high-precision charged-particle tracking system for measuring momenta [26,27]; two ring-imaging Cherenkov detectors for distinguishing charged hadrons [28]; a calorimeter system for identifying photons, electrons, and hadrons; and a system for identifying muons [29]. The trigger consists of a hardware stage, based on information from the calorimeter and muon systems, followed by a software stage, which applies a full event reconstruction [30]. The selection of $B^0 \to K^{*0}\chi$ candidates in the software trigger requires the presence of a vertex identified by a multivariate algorithm [31] as being consistent with the decay of a $b$ hadron. Alternatively, candidates may be selected based on the presence of a displaced dimuon vertex, or the presence of a muon with large transverse momentum ($p_T$) and large impact parameter (IP), defined as the minimum track distance with respect to any $pp$-interaction vertex (PV). Only tracks with segments reconstructed in the first charged-particle detector, which surrounds the interaction region and is about 1 m in length [26], can satisfy these trigger requirements; therefore, the $\chi$ boson is required to decay well within this detector. In the simulation, $pp$ collisions are generated following Refs. [32–35], and the interactions of the outgoing particles with the detector are modeled as in Refs. [36,37].

A search is conducted, following Ref. [38], by scanning the $m(\mu^+\mu^-)$ distribution for an excess of $\chi$ signal candidates over the expected background. In order to avoid experimenter bias, all aspects of the search are fixed without examining those $B^0 \to K^{*0}\chi$ candidates which have an invariant mass consistent with the known $B^0$ mass [39]. The step sizes in $m(\chi)$ are $\sigma[m(\mu^+\mu^-)]/2$, where $\sigma[m(\mu^+\mu^-)]$ is the dimuon mass resolution. Signal candidates satisfy $|m(\mu^+\mu^-) - m(\chi)| < 2\sigma[m(\mu^+\mu^-)]$, while the background is estimated by interpolating the yields in the sidebands starting at $3\sigma[m(\mu^+\mu^-)]$ from $m(\chi)$ . With $m(K^+\pi^-\mu^+\mu^-)$ constrained [40] to the known $B^0$ mass, $\sigma[m(\mu^+\mu^-)]$ is less than 8 MeV over the entire $m(\mu^+\mu^-)$ range, and is as small as 2 MeV below 220 MeV . The statistical test at each $m(\chi)$ is based on the profile likelihood ratio of Poisson-process hypotheses with and without a signal contribution [41]. The uncertainty on the background interpolation is modeled by a Gaussian term in the likelihood (see Ref. [38] for details).

The $\chi \to \mu^+\mu^-$ decay vertex is permitted, but not required, to be displaced from the $B^0 \to K^{*0}\chi$ decay vertex. Two regions of reconstructed dimuon lifetime, $\tau(\mu^+\mu^-)$, are defined for each $m(\chi)$ considered in the search: a prompt region, $|\tau(\mu^+\mu^-)| < 3\sigma[\tau(\mu^+\mu^-)]$, and a displaced region, $\tau(\mu^+\mu^-) > 3\sigma[\tau(\mu^+\mu^-)]$. The lifetime resolution is about 0.2 ps for $m(\mu^+\mu^-) \gtrsim 250$ MeV, and 1 ps near $2m(\mu)$. The joint likelihood is formed from the product of the likelihoods for candidates populating the prompt and displaced regions, since no assumption is made about $\tau(\chi)$ . Narrow resonances are vetoed by excluding the regions near the $\omega$, $\phi$, $J/\psi$, $\psi(2S)$, and $\psi(3770)$ resonances. These regions are removed in both the prompt and displaced samples to avoid contamination from unassociated dimuon and $K^{*0}$ resonances.

The branching fraction product $\mathcal{B}(B^0 \to K^{*0}\chi(\mu^+\mu^-)) \equiv \mathcal{B}(B^0 \to K^{*0}\chi) \times \mathcal{B}(\chi \to \mu^+\mu^-)$ is measured relative to $\mathcal{B}(B^0 \to K^{*0}\mu^+\mu^-)$, where the normalization sample is taken from the prompt region and restricted to $1.1 < m^2(\mu^+\mu^-) < 6.0$ GeV$^2$. This normalization decay is chosen since the detector response is similar to that for the $B^0 \to K^{*0}\chi$ decay, and because the hidden-sector theory parameters can be obtained from the ratio $\mathcal{B}(B^0 \to K^{*0}\chi(\mu^+\mu^-))/\mathcal{B}(B^0 \to K^{*0}\mu^+\mu^-)$ with reduced theoretical uncertainty. Correlations between the yields of a possible signal in the prompt $1.1 < m^2(\mu^+\mu^-) < 6.0$ GeV$^2$ region and the normalization decay are at most a few percent and are ignored.

The selection is similar to that of Ref. [42] with the exception that the $K^{*0}$ and dimuon candidates are not required to share a common vertex. Signal candidates are required to satisfy a set of loose requirements: the $B^0$, $K^{*0}$, and $\chi$ decay vertices must all be separated from any PV and be of good quality; the $B^0$ IP must be small, while the IP of the kaon, pion, and muons must be large; the angle between the $B^0$ momentum vector and the vector between the associated PV and the $B^0$ decay vertex must be small; and the kaon, pion, and muons must each satisfy loose particle identification requirements. Candidates are retained if $m(K^+\pi^-)$ is within 100 MeV of the known $K^{*0}$ mass [39].

A multivariate selection is applied to reduce the background further. The uBoost algorithm [43] is employed to ensure that the performance is nearly independent of $m(\chi)$ and $\tau(\chi)$ . The inputs to the algorithm include $p_T(B^0)$, various topological features of the decay, the muon identification quality, and an isolation criterion [44] designed to suppress backgrounds from partially reconstructed decays. Data from the high-mass sideband, $150 < m(K^+\pi^-\mu^+\mu^-) - m(B^0) < 500$ MeV, are used to represent the background in the training, while simulated samples generated with $m(\chi)$ values of 214, 1000, and 4000 MeV, and $\tau(\chi)$ large enough to populate the full

reconstructible region, are used for the signal. The multivariate selection requirement is determined by maximizing the figure of merit of Ref. [45] for finding a signal with a significance of 5 standard deviations. This results in a signal selection efficiency of 85% with a background rejection of 92% on average. The uBoost algorithm is validated using ten additional signal samples generated with various other $m(\chi)$ and $\tau(\chi)$ values. The performance is consistent for all samples.

Peaking backgrounds that survive the multivariate selection are vetoed explicitly. A small number of $B_s^0 \to \phi(K^+K^-)\mu^+\mu^-$ decays are removed by rejecting $K^+\pi^-$ candidates that are consistent with the decay $\phi \to K^+K^-$ if the $\pi^-$ is assumed to be a misidentified $K^-$. A similar veto is applied that removes about 250 $\Lambda_b^0 \to pK^-\mu^+\mu^-$ decays. Candidates are also rejected if the dimuon system is consistent with any of the following decays: $K_S^0 \to \pi^+\pi^-$, where the pions decay in flight to muons; $\Lambda^0 \to p\pi^-$, where the pion decays in flight and the proton is misidentified as a muon; and $\bar{D}^0 \to K^+\pi^-$, where the kaon and pion decay in flight. All other particle-misidentification backgrounds are negligible.

Figure 2 shows the $K^+\pi^-\mu^+\mu^-$ mass distribution for all prompt candidates that satisfy the full selection in the region $1.1 < m^2(\mu^+\mu^-) < 6.0$ GeV$^2$. An unbinned extended maximum likelihood fit is performed to obtain the $B^0 \to K^{*0}\mu^+\mu^-$ yield. The signal model is obtained from data using the subset of prompt candidates with $m(\mu^+\mu^-)$ in the $J/\psi$ region, where the background is $\mathcal{O}(10^{-3})$. A small correction, obtained from simulation, is applied to account for the difference in signal shape expected in the $1.1 < m^2(\mu^+\mu^-) < 6.0$ GeV$^2$ region. The background model is an exponential function. Several alternative background models are considered, with the largest shift observed in the signal yield (1%) assigned as a systematic uncertainty. The $S$-wave fraction (i.e., not a $K^{*0}$ meson) of the $K\pi$ system within the selected $K\pi$ mass range is $(4 \pm 4)\%$ [42]. The yield of the normalization mode is

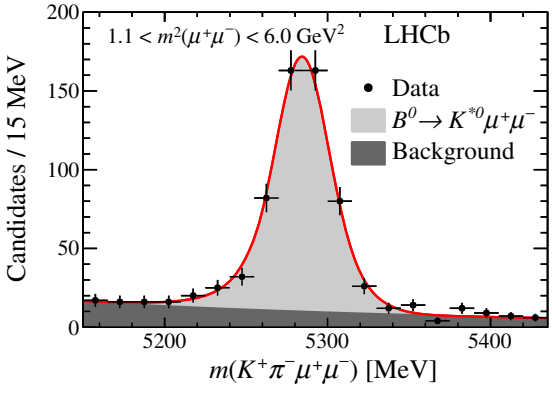


FIG. 2 (color online). Invariant mass spectrum with fit overlaid for all prompt $B^0 \to K^{*0}\mu^+\mu^-$ candidates with $1.1 < m^2(\mu^+\mu^-) < 6.0$ GeV$^2$.

$N(B^0 \to K^{*0}\mu^+\mu^-) = 506 \pm 33$, where the uncertainty includes both statistical and systematic contributions.

Probability density functions, obtained from the data using splines, are used to generate simulated data sets under the no-signal hypothesis from which the global significance of any $\chi$ signal is obtained [38]. For this the data are collected in the prompt region into wide bins with a width of 200 MeV, and into a total of three bins in the displaced region. Simulated events show that the presence of a narrow $\chi$ signal anywhere in the $m(\chi)$-$\tau(\chi)$ plane, whose local significance is $5\sigma$, would not produce a significant excess in these wide-binned data.

Figure 3 shows the $m(\mu^+\mu^-)$ distributions in both the prompt and displaced regions for candidates whose invariant mass is within 50 MeV of the known $B^0$ mass. The most significant local excess occurs for $m(\chi) = 253$ MeV, where in the prompt region 11 (6.2) candidates are observed (expected), while the displaced region contains a single candidate which is the only displaced candidate below $m(\omega)$. The $p$ value of the no-signal hypothesis is about 80%, showing that no evidence is found for a hidden-sector boson.

To set upper limits on $\mathcal{B}(B^0 \to K^{*0}\chi(\mu^+\mu^-))$, various sources of systematic uncertainty are considered. The limits are set using the profile likelihood technique [46], in which systematic uncertainties are handled by including additional Gaussian terms in the likelihood [38]. Since no contamination from the $\omega$ or $\phi$ resonance is found in the displaced region, upper limits are set in these $m(\chi)$ regions for $\tau(\chi) > 1$ ps.

Many uncertainties cancel to a good approximation because the signal and normalization decays share the same final state. The dominant uncertainty on the efficiency ratio $\epsilon(B^0 \to K^{*0}\chi(\mu^+\mu^-))/\epsilon(B^0 \to K^{*0}\mu^+\mu^-)$, which is taken from simulation, arises due to its dependence on $\tau(\mu^+\mu^-)$. The simulation is validated by comparing $\tau(\pi^+\pi^-)$ distributions between $B^0 \to J/\psi K_S^0(\pi^+\pi^-)$ decays reconstructed in simulated and experimental data in bins of $K_S^0$ momentum. The distributions in data and simulation are consistent in each bin, and the per-bin statistical precision (5%) is assigned as systematic uncertainty.

The uncertainty on the efficiency for a signal candidate to be reconstructed within a given $m(\mu^+\mu^-)$ signal window, due to mismodeling of $\sigma[m(\mu^+\mu^-)]$, is determined to be 1% based on a comparison of the $J/\psi$ peak between $B^0 \to J/\psi(\mu^+\mu^-)K^{*0}$ decays in simulated and experimental data. A similar comparison for $\sigma[\tau(\mu^+\mu^-)]$ shows that the uncertainty on the fraction of signal candidates expected to be reconstructed in the prompt and displaced regions is negligible. Finally, the efficiency for the normalization mode is determined using the measured angular distribution [47], which is varied within the uncertainties yielding an uncertainty in the normalization-mode efficiency of 1%. The individual contributions are summed in quadrature giving a total systematic uncertainty of 8%.

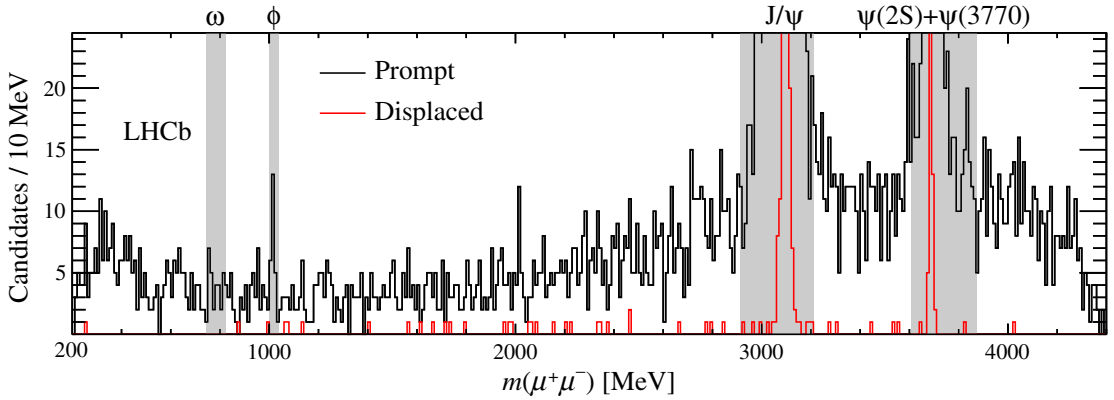


FIG. 3 (color online). Distribution of $m(\mu^+\mu^-)$ in the (black) prompt and (red) displaced regions. The shaded bands denote regions where no search is performed due to (possible) resonance contributions. The $J/\psi$, $\psi(2S)$, and $\psi(3770)$ peaks are suppressed to better display the search region.

The spin of the hidden-sector boson determines the angular distribution of the decay and, therefore, affects the efficiency. The upper limits are set assuming spin zero. For a spin-one $\chi$ boson produced unpolarized in the decay, the sensitivity is about 10%–20% better than for the spin-zero case. The dependence on the polarization in the spin-one case is provided in the Supplemental Material [48].

Figure 4 shows the upper limits on $\mathcal{B}(B^0 \to K^{*0}\chi(\mu^+\mu^-))$, relative to $\mathcal{B}(B^0 \to K^{*0}\mu^+\mu^-)$ in the $1.1 < m^2(\mu^+\mu^-) < 6.0\ \mathrm{GeV}^2$ region, set at the 95% confidence level (C.L.) for several values of $\tau(\chi)$; limits as functions of $\tau(\chi)$ are provided in the Supplemental Material [48]. The limits become less stringent for $\tau(\chi) \gtrsim 10$ ps, as the probability of the $\chi$ boson decaying within the first charged-particle detector decreases. The branching fraction $\mathcal{B}(B^0 \to K^{*0}\mu^+\mu^-) = (1.6 \pm 0.3) \times 10^{-7}$ [42] is used to obtain upper limits on $\mathcal{B}(B^0 \to K^{*0}\chi(\mu^+\mu^-))$, which are also shown in Fig. 4. Because of the uncertainty on the normalization-mode branching fraction, there is not a one-to-one mapping between the two axes in the figure; however, the absolute limits shown are accurate to about 2%.

Figure 5 shows exclusion regions for the DFSZ [49,50] axion model of Ref. [20] set in the limit of the large ratio of Higgs-doublet vacuum expectation values, $\tan\beta \gtrsim 3$, for charged-Higgs masses $m(h) = 1$ and 10 TeV (this choice of restricted parameter space is made for ease of graphical presentation). The constraints scale as $\log[m(h)/\mathrm{TeV}]$ for $m(h) \gtrsim 800$ GeV. The branching fraction of the axion into hadrons varies greatly in different models. Figure 5 shows the results for two extreme cases: $\mathcal{B}(\chi \to \text{hadrons}) = 0$ and 0.99. While $\mathcal{B}(\chi \to \mu^+\mu^-)$ is 100 times larger when $\mathcal{B}(\chi \to \text{hadrons}) = 0$, $\tau(\chi)$ is also larger, which results in the model probing the region where the upper limits are weaker. The constraints are loose for $m(\chi) > 2m(\tau)$, since the axion preferentially decays into $\tau^+\tau^-$ if kinematically allowed; otherwise the exclusions reach the PeV scale.

Figure 5 also shows exclusion regions for the inflaton model of Ref. [51], which only considers $m(\chi) < 1$ GeV. The branching fraction into hadrons is taken directly from

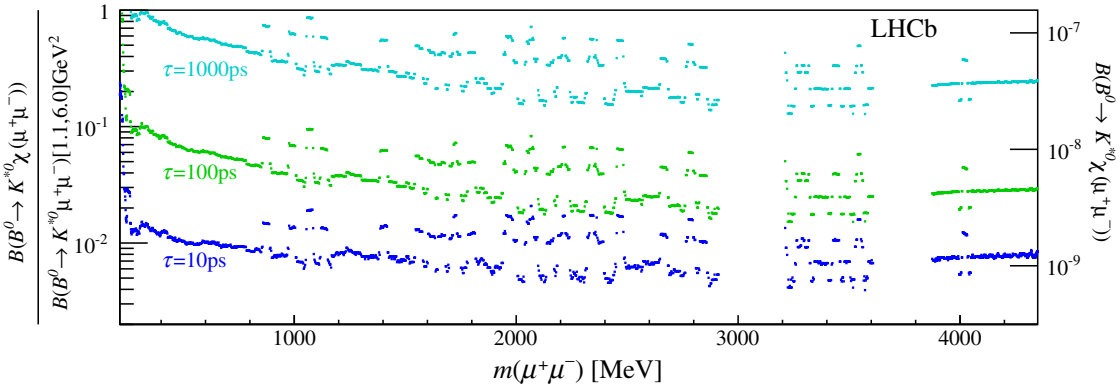


FIG. 4 (color online). Upper limits at 95% C.L. for (left axis) $\mathcal{B}(B^0 \to K^{*0}\chi(\mu^+\mu^-))/\mathcal{B}(B^0 \to K^{*0}\mu^+\mu^-)$, with $B^0 \to K^{*0}\mu^+\mu^-$ in $1.1 < m^2(\mu^+\mu^-) < 6.0\ \mathrm{GeV}^2$, and (right axis) $\mathcal{B}(B^0 \to K^{*0}\chi(\mu^+\mu^-))$. The sparseness of the data leads to rapid fluctuations in the limits. Excluding the region near $2m(\mu)$, the relative limits for $\tau < 10$ ps are between 0.005–0.05 and all relative limits for $\tau \leq 1000$ ps are less than 1.

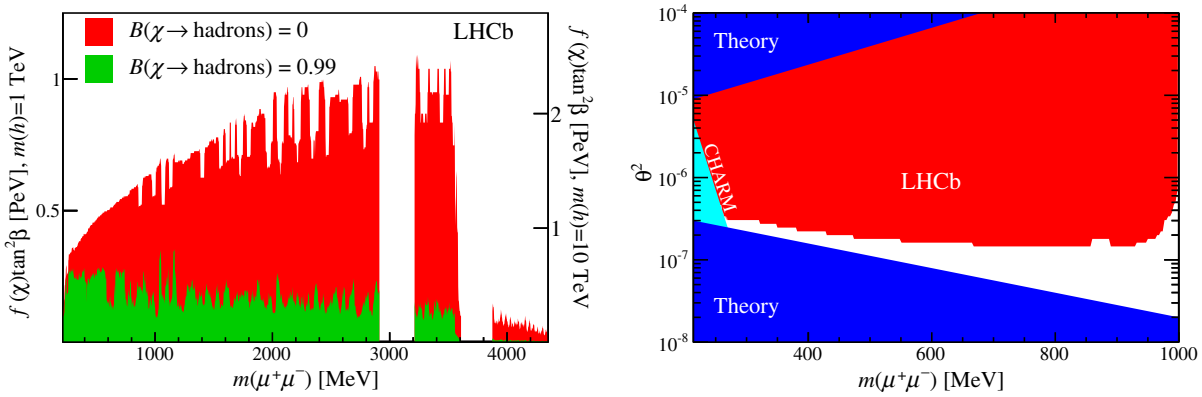


FIG. 5 (color online). Exclusion regions at 95% C.L.: (left) constraints on the axion model of Ref. [20]; (right) constraints on the inflaton model of Ref. [51]. The regions excluded by the theory [51] and by the CHARM experiment [52] are also shown.

Ref. [51] and, as in the axion model, is highly uncertain but this does not greatly affect the sensitivity of this search. Constraints are placed on the mixing angle between the Higgs and inflaton fields, $\theta$, which exclude most of the previously allowed region.

In summary, no evidence for a signal is observed, and upper limits are placed on $\mathcal{B}(B^0 \to K^{*0}\chi) \times \mathcal{B}(\chi \to \mu^+\mu^-)$. This is the first dedicated search over a large mass range for a hidden-sector boson in a decay mediated by a $b \to s$ transition at leading order, and the most sensitive search to date over the entire accessible mass range. Stringent constraints are placed on theories that predict the existence of additional scalar or axial-vector fields.

We express our gratitude to our colleagues in the CERN accelerator departments for the excellent performance of the LHC. We thank the technical and administrative staff at the LHCb institutes. We acknowledge support from CERN and from the following national agencies: CAPES, CNPq, FAPERJ, and FINEP (Brazil); NSFC (China); CNRS/IN2P3 (France); BMBF, DFG, HGF, and MPG (Germany); INFN (Italy); FOM and NWO (Netherlands); MNiSW and NCN (Poland); MEN/IFA (Romania); MinES and FANO (Russia); MinECo (Spain); SNSF and SER (Switzerland); NASU (Ukraine); STFC (United Kingdom); NSF (USA). The Tier1 computing centers are supported by IN2P3 (France), KIT and BMBF (Germany), INFN (Italy), NWO and SURF (Netherlands), PIC (Spain), GridPP (United Kingdom). We are indebted to the communities behind the multiple open source software packages on which we depend. We are also thankful for the computing resources and the access to software R&D tools provided by Yandex LLC (Russia). Individual groups or members have received support from EPLANET, Marie Skłodowska-Curie Actions, and ERC (European Union), Conseil général de Haute-Savoie, Labex ENIGMASS and OCEVU, Région Auvergne (France), RFBR (Russia), XuntaGal and GENCAT (Spain), Royal Society and Royal Commission for the Exhibition of 1851 (United Kingdom).

[1] R. Essig *et al.*, Dark Sectors and New, Light, Weakly-Coupled Particles, arXiv:1311.0029.
[2] G. Weidenspointner *et al.*, The sky distribution of positronium annihilation continuum emission measured with SPI/INTEGRAL, Astron. Astrophys. **450**, 1013 (2006).
[3] J. Chang *et al.*, An excess of cosmic ray electrons at energies of 300–800 GeV, Nature (London) **456**, 362 (2008).
[4] O. Adriani *et al.* (PAMELA Collaboration), An anomalous positron abundance in cosmic rays with energies 1.5–100 GeV, Nature (London) **458**, 607 (2009).
[5] O. Adriani *et al.* (PAMELA Collaboration), Cosmic-ray electron flux measured by the PAMELA experiment between 1 and 625 GeV, Phys. Rev. Lett. **106**, 201101 (2011).
[6] O. Adriani *et al.* (PAMELA Collaboration), Cosmic-ray positron energy spectrum measured by PAMELA, Phys. Rev. Lett. **111**, 081102 (2013) .
[7] M. Ackermann *et al.* (Fermi LAT Collaboration), Measurement of separate cosmic-ray electron and positron spectra with the Fermi Large Area Telescope, Phys. Rev. Lett. **108**, 011103 (2012).
[8] M. Aguilar *et al.* (AMS Collaboration), Electron and positron fluxes in primary cosmic rays measured with the Alpha Magnetic Spectrometer on the International Space Station, Phys. Rev. Lett. **113**, 121102 (2014).
[9] N. Arkani-Hamed, D. P. Finkbeiner, T. R. Slatyer, and N. Weiner, A theory of dark matter, Phys. Rev. D **79**, 015014 (2009).
[10] M. Pospelov and A. Ritz, Astrophysical signatures of secluded dark matter, Phys. Lett. B **671**, 391 (2009).
[11] C. Cheung, J. T. Ruderman, L.-T. Wang, and I. Yavin, Kinetic mixing as the origin of a light dark-gauge-group scale, Phys. Rev. D **80**, 035008 (2009).
[12] S. Alekhin *et al.*, A facility to Search for Hidden Particles at the CERN SPS: the SHiP physics case, arXiv:1504.04855.
[13] F. Bezrukov and D. Gorbunov, Light inflaton hunter's guide, J. High Energy Phys. 05 (2010) 010.

[14] M. P. Hertzberg and J. Karouby, Generating the observed baryon asymmetry from the inflaton field, Phys. Rev. D **89**, 063523 (2014).
[15] M. P. Hertzberg and J. Karouby, Baryogenesis from the inflaton field, Phys. Lett. B **737**, 34 (2014).
[16] R. D. Peccei, The strong *CP* problem and axions, Lect. Notes Phys. **741**, 3 (2008).
[17] R. D. Peccei and H. R. Quinn, *CP* conservation in the presence of pseudoparticles, Phys. Rev. Lett. **38**, 1440 (1977).
[18] Y. Nomura and J. Thaler, Dark matter through the axion portal, Phys. Rev. D **79**, 075008 (2009).
[19] J. Mardon, Y. Nomura, and J. Thaler, Cosmic signals from the hidden sector, Phys. Rev. D **80**, 035013 (2009).
[20] M. Freytsis, Z. Ligeti, and J. Thaler, Constraining the axion portal with $B \to K\ell^+\ell^-$, Phys. Rev. D **81**, 034001 (2010).
[21] D. Hooper and T. M. P. Tait, Neutralinos in an extension of the minimal supersymmetric standard model as the source of the PAMELA positron excess, Phys. Rev. D **80**, 055028 (2009).
[22] H. J. Hyun *et al.* (Belle Collaboration), Search for a low mass particle decaying into $\mu^+\mu^-$ in $B^0 \to K^{*0}X$ and $B^0 \to \rho^0 X$ at Belle, Phys. Rev. Lett. **105**, 091801 (2010).
[23] J. P. Lees *et al.* (*BaBar* Collaboration), Search for long-lived particles in $e^+e^-$ collisions, Phys. Rev. Lett. **114**, 171801 (2015).
[24] A. A. Alves Jr. *et al.* (LHCb Collaboration), The LHCb detector at the LHC, JINST **3**, S08005 (2008).
[25] R. Aaij *et al.* (LHCb Collaboration), LHCb detector performance, Int. J. Mod. Phys. A **30**, 1530022 (2015).
[26] R. Aaij *et al.*, Performance of the LHCb Vertex Locator, JINST **9**, P09007 (2014).
[27] R. Arink *et al.*, Performance of the LHCb Outer Tracker, JINST **9**, P01002 (2014).
[28] M. Adinolfi *et al.*, Performance of the LHCb RICH detector at the LHC, Eur. Phys. J. C **73**, 2431 (2013).
[29] A. A. Alves Jr. *et al.*, Performance of the LHCb muon system, JINST **8**, P02022 (2013).
[30] R. Aaij *et al.*, The LHCb trigger and its performance in 2011, JINST **8**, P04022 (2013).
[31] V. V. Gligorov and M. Williams, Efficient, reliable and fast high-level triggering using a bonsai boosted decision tree, JINST **8**, P02013 (2013).
[32] T. Sjöstrand, S. Mrenna, and P. Skands, A brief introduction to PYTHIA 8.1, Comput. Phys. Commun. **178**, 852 (2008).
[33] I. Belyaev *et al.*, Handling of the generation of primary events in Gauss, the LHCb simulation framework, J. Phys. Conf. Ser. **331**, 032047 (2011).
[34] D. J. Lange, The EvtGen particle decay simulation package, Nucl. Instrum. Methods Phys. Res., Sect. A **462**, 152 (2001).
[35] P. Golonka and Z. Was, PHOTOS Monte Carlo: A precision tool for QED corrections in $Z$ and $W$ decays, Eur. Phys. J. C **45**, 97 (2006).
[36] J. Allison *et al.* (Geant4 Collaboration), Geant4 developments and applications, IEEE Trans. Nucl. Sci. **53**, 270 (2006); S. Agostinelli *et al.* (Geant4 Collaboration), Geant4: A simulation toolkit, Nucl. Instrum. Methods Phys. Res., Sect. A **506**, 250 (2003).
[37] M. Clemencic, G. Corti, S. Easo, C. R. Jones, S. MiglioranziM. Pappagallo, and P. Robbe, The LHCb simulation application, Gauss: Design, evolution and experience, J. Phys. Conf. Ser. **331**, 032023 (2011).
[38] M. Williams, Searching for a particle of unknown mass and lifetime in the presence of an unknown non-monotonic background, JINST **10**, P06002 (2015).
[39] K. A. Olive *et al.* (Particle Data Group), Review of particle physics, Chin. Phys. C **38**, 090001 (2014).
[40] W. D. Hulsbergen, Decay chain fitting with a Kalman filter, Nucl. Instrum. Methods Phys. Res., Sect. A **552**, 566 (2005).
[41] G. Cowan, K. Cranmer, E. Gross, and O. Vitells, Asymptotic formulae for likelihood-based tests of new physics, Eur. Phys. J. C **71**, 1554 (2011).
[42] R. Aaij *et al.* (LHCb Collaboration), Differential branching fraction and angular analysis of the decay $B^0 \to K^{*0}\mu^+\mu^-$, J. High Energy Phys. 08 (2013) 131.
[43] J. Stevens and M. Williams, uBoost: A boosting method for producing uniform selection efficiencies from multivariate classifiers, JINST **8**, P12013 (2013).
[44] R. Aaij *et al.* (LHCb Collaboration), Measurement of the Ratio of Branching Fractions $\mathcal{B}(\bar{B}^0 \to D^{*+}\tau^-\bar{\nu}_\tau)/\mathcal{B}(\bar{B}^0 \to D^{*+}\mu^-\bar{\nu}_\mu)$, Phys. Rev. Lett. **115**, 111803 (2015).
[45] G. Punzi, Sensitivity of searches for new signals and its optimization, arXiv:physics/0308063.
[46] W. A. Rolke, A. M. Lopez, and J. Conrad, Limits and confidence intervals in the presence of nuisance parameters, Nucl. Instrum. Methods Phys. Res., Sect. A **551**, 493 (2005).
[47] LHCb Collaboration, Report No. LHCb-CONF-2015-002 (2015).
[48] See Supplemental Material at http://link.aps.org/supplemental/10.1103/PhysRevLett.115.161802 for upper limits as functions of $\tau(\chi)$, and for instructions on how to convert these into limits for a spin-one boson.
[49] M. Dine, W. Fischler, and M. Srednicki, A simple solution to the strong *CP* problem with a harmless axion, Phys. Lett. B **104**, 199 (1981).
[50] A. R. Zhitnitsky, On possible suppression of the axion hadron interactions, Sov. J. Nucl. Phys. **31**, 260 (1980).
[51] F. Bezrukov and D. Gorbunov, Relic gravity waves and 7 keV dark matter from a GeV scale inflaton, Phys. Lett. B **736**, 494 (2014).
[52] F. Bergsma *et al.* (CHARM Collaboration), Search for axion like particle production in 400 GeV proton-copper interactions, Phys. Lett. B **157**, 458 (1985).

R. Aaij,[38] B. Adeva,[37] M. Adinolfi,[46] A. Affolder,[52] Z. Ajaltouni,[5] S. Akar,[6] J. Albrecht,[9] F. Alessio,[38] M. Alexander,[51] S. Ali,[41] G. Alkhazov,[30] P. Alvarez Cartelle,[53] A. A. Alves Jr,[57] S. Amato,[2] S. Amerio,[22] Y. Amhis,[7] L. An,[3] L. Anderlini,[17]

J. Anderson,[40] G. Andreassi,[39] M. Andreotti,[16,a] J. E. Andrews,[58] R. B. Appleby,[54] O. Aquines Gutierrez,[10] F. Archilli,[38] P. d'Argent,[11] A. Artamonov,[35] M. Artuso,[59] E. Aslanides,[6] G. Auriemma,[25,b] M. Baalouch,[5] S. Bachmann,[11] J. J. Back,[48] A. Badalov,[36] C. Baesso,[60] W. Baldini,[16,38] R. J. Barlow,[54] C. Barschel,[38] S. Barsuk,[7] W. Barter,[38] V. Batozskaya,[28] V. Battista,[39] A. Bay,[39] L. Beaucourt,[4] J. Beddow,[51] F. Bedeschi,[23] I. Bediaga,[1] L. J. Bel,[41] V. Bellee,[39] N. Belloli,[20] I. Belyaev,[31] E. Ben-Haim,[8] G. Bencivenni,[18] S. Benson,[38] J. Benton,[46] A. Berezhnoy,[32] R. Bernet,[40] A. Bertolin,[22] M.-O. Bettler,[38] M. van Beuzekom,[41] A. Bien,[11] S. Bifani,[45] P. Billoir,[8] T. Bird,[54] A. Birnkraut,[9] A. Bizzeti,[17,c] T. Blake,[48] F. Blanc,[39] J. Blouw,[10] S. Blusk,[59] V. Bocci,[25] A. Bondar,[34] N. Bondar,[30,38] W. Bonivento,[15] S. Borghi,[54] M. Borsato,[7] T. J. V. Bowcock,[52] E. Bowen,[40] C. Bozzi,[16] S. Braun,[11] M. Britsch,[10] T. Britton,[59] J. Brodzicka,[54] N. H. Brook,[46] E. Buchanan,[46] A. Bursche,[40] J. Buytaert,[38] S. Cadeddu,[15] R. Calabrese,[16,a] M. Calvi,[20,d] M. Calvo Gomez,[36,e] P. Campana,[18] D. Campora Perez,[38] L. Capriotti,[54] A. Carbone,[14,f] G. Carboni,[24,g] R. Cardinale,[19,h] A. Cardini,[15] P. Carniti,[20] L. Carson,[50] K. Carvalho Akiba,[2,38] G. Casse,[52] L. Cassina,[20,d] L. Castillo Garcia,[38] M. Cattaneo,[38] Ch. Cauet,[9] G. Cavallero,[19] R. Cenci,[23,i] M. Charles,[8] Ph. Charpentier,[38] M. Chefdeville,[4] S. Chen,[54] S.-F. Cheung,[55] N. Chiapolini,[40] M. Chrzaszcz,[40] X. Cid Vidal,[38] G. Ciezarek,[41] P. E. L. Clarke,[50] M. Clemencic,[38] H. V. Cliff,[47] J. Closier,[38] V. Coco,[38] J. Cogan,[6] E. Cogneras,[5] V. Cogoni,[15,j] L. Cojocariu,[29] G. Collazuol,[22] P. Collins,[38] A. Comerma-Montells,[11] A. Contu,[15] A. Cook,[46] M. Coombes,[46] S. Coquereau,[8] G. Corti,[38] M. Corvo,[16,a] B. Couturier,[38] G. A. Cowan,[50] D. C. Craik,[48] A. Crocombe,[48] M. Cruz Torres,[60] S. Cunliffe,[53] R. Currie,[53] C. D'Ambrosio,[38] E. Dall'Occo,[41] J. Dalseno,[46] P. N. Y. David,[41] A. Davis,[57] K. De Bruyn,[41] S. De Capua,[54] M. De Cian,[11] J. M. De Miranda,[1] L. De Paula,[2] P. De Simone,[18] C.-T. Dean,[51] D. Decamp,[4] M. Deckenhoff,[9] L. Del Buono,[8] N. Déléage,[4] M. Demmer,[9] D. Derkach,[55] O. Deschamps,[5] F. Dettori,[38] B. Dey,[21] A. Di Canto,[38] F. Di Ruscio,[24] H. Dijkstra,[38] S. Donleavy,[52] F. Dordei,[11] M. Dorigo,[39] A. Dosil Suárez,[37] D. Dossett,[48] A. Dovbnya,[43] K. Dreimanis,[52] L. Dufour,[41] G. Dujany,[54] F. Dupertuis,[39] P. Durante,[38] R. Dzhelyadin,[35] A. Dziurda,[26] A. Dzyuba,[30] S. Easo,[49,38] U. Egede,[53] V. Egorychev,[31] S. Eidelman,[34] S. Eisenhardt,[50] U. Eitschberger,[9] R. Ekelhof,[9] L. Eklund,[51] I. El Rifai,[5] Ch. Elsasser,[40] S. Ely,[59] S. Esen,[11] H. M. Evans,[47] T. Evans,[55] A. Falabella,[14] C. Färber,[38] N. Farley,[45] S. Farry,[52] R. Fay,[52] D. Ferguson,[50] V. Fernandez Albor,[37] F. Ferrari,[14] F. Ferreira Rodrigues,[1] M. Ferro-Luzzi,[38] S. Filippov,[33] M. Fiore,[16,38,a] M. Fiorini,[16,a] M. Firlej,[27] C. Fitzpatrick,[39] T. Fiutowski,[27] K. Fohl,[38] P. Fol,[53] M. Fontana,[15] F. Fontanelli,[19,h] R. Forty,[38] O. Francisco,[2] M. Frank,[38] C. Frei,[38] M. Frosini,[17] J. Fu,[21] E. Furfaro,[24,g] A. Gallas Torreira,[37] D. Galli,[14,f] S. Gallorini,[22] S. Gambetta,[50] M. Gandelman,[2] P. Gandini,[55] Y. Gao,[3] J. García Pardiñas,[37] J. Garra Tico,[47] L. Garrido,[36] D. Gascon,[36] C. Gaspar,[38] R. Gauld,[55] L. Gavardi,[9] G. Gazzoni,[5] D. Gerick,[11] E. Gersabeck,[11] M. Gersabeck,[54] T. Gershon,[48] Ph. Ghez,[4] A. Gianelle,[22] S. Gianì,[39] V. Gibson,[47] O. G. Girard,[39] L. Giubega,[29] V. V. Gligorov,[38] C. Göbel,[60] D. Golubkov,[31] A. Golutvin,[53,38] A. Gomes,[1,k] C. Gotti,[20,d] M. Grabalosa Gándara,[5] R. Graciani Diaz,[36] L. A. Granado Cardoso,[38] E. Graugés,[36] E. Graverini,[40] G. Graziani,[17] A. Grecu,[29] E. Greening,[55] S. Gregson,[47] P. Griffith,[45] L. Grillo,[11] O. Grünberg,[63] B. Gui,[59] E. Gushchin,[33] Yu. Guz,[35,38] T. Gys,[38] T. Hadavizadeh,[55] C. Hadjivasiliou,[59] G. Haefeli,[39] C. Haen,[38] S. C. Haines,[47] S. Hall,[53] B. Hamilton,[58] X. Han,[11] S. Hansmann-Menzemer,[11] N. Harnew,[55] S. T. Harnew,[46] J. Harrison,[54] J. He,[38] T. Head,[39] V. Heijne,[41] K. Hennessy,[52] P. Henrard,[5] L. Henry,[8] J. A. Hernando Morata,[37] E. van Herwijnen,[38] M. Heß,[63] A. Hicheur,[2] D. Hill,[55] M. Hoballah,[5] C. Hombach,[54] W. Hulsbergen,[41] T. Humair,[53] N. Hussain,[55] D. Hutchcroft,[52] D. Hynds,[51] M. Idzik,[27] P. Ilten,[56] R. Jacobsson,[38] A. Jaeger,[11] J. Jalocha,[55] E. Jans,[41] A. Jawahery,[58] F. Jing,[3] M. John,[55] D. Johnson,[38] C. R. Jones,[47] C. Joram,[38] B. Jost,[38] N. Jurik,[59] S. Kandybei,[43] W. Kanso,[6] M. Karacson,[38] T. M. Karbach,[38] S. Karodia,[51] M. Kecke,[11] M. Kelsey,[59] I. R. Kenyon,[45] M. Kenzie,[38] T. Ketel,[42] E. Khairullin,[65] B. Khanji,[20,38,d] C. Khurewathanakul,[39] S. Klaver,[54] K. Klimaszewski,[28] O. Kochebina,[7] M. Kolpin,[11] I. Komarov,[39] R. F. Koopman,[42] P. Koppenburg,[41,38] M. Kozeiha,[5] L. Kravchuk,[33] K. Kreplin,[11] M. Kreps,[48] G. Krocker,[11] P. Krokovny,[34] F. Kruse,[9] W. Krzemien,[28] W. Kucewicz,[26,l] M. Kucharczyk,[26] V. Kudryavtsev,[34] A. K. Kuonen,[39] K. Kurek,[28] T. Kvaratskheliya,[31] D. Lacarrere,[38] G. Lafferty,[54] A. Lai,[15] D. Lambert,[50] G. Lanfranchi,[18] C. Langenbruch,[48] B. Langhans,[38] T. Latham,[48] C. Lazzeroni,[45] R. Le Gac,[6] J. van Leerdam,[41] J.-P. Lees,[4] R. Lefèvre,[5] A. Leflat,[32,38] J. Lefrançois,[7] E. Lemos Cid,[37] O. Leroy,[6] T. Lesiak,[26] B. Leverington,[11] Y. Li,[7] T. Likhomanenko,[65,64] M. Liles,[52] R. Lindner,[38] C. Linn,[38] F. Lionetto,[40] B. Liu,[15] X. Liu,[3] D. Loh,[48] I. Longstaff,[51] J. H. Lopes,[2] D. Lucchesi,[22,m] M. Lucio Martinez,[37] H. Luo,[50] A. Lupato,[22] E. Luppi,[16,a] O. Lupton,[55] A. Lusiani,[23] F. Machefert,[7] F. Maciuc,[29] O. Maev,[30] K. Maguire,[54] S. Malde,[55] A. Malinin,[64] G. Manca,[7] G. Mancinelli,[6] P. Manning,[59] A. Mapelli,[38] J. Maratas,[5] J. F. Marchand,[4] U. Marconi,[14] C. Marin Benito,[36] P. Marino,[23,38,i] J. Marks,[11] G. Martellotti,[25] M. Martin,[6] M. Martinelli,[39] D. Martinez Santos,[37] F. Martinez Vidal,[66] D. Martins Tostes,[2] A. Massafferri,[1] R. Matev,[38] A. Mathad,[48] Z. Mathe,[38] C. Matteuzzi,[20] A. Mauri,[40] B. Maurin,[39] A. Mazurov,[45]

M. McCann,[53] J. McCarthy,[45] A. McNab,[54] R. McNulty,[12] B. Meadows,[57] F. Meier,[9] M. Meissner,[11] D. Melnychuk,[28] M. Merk,[41] E Michielin,[22] D. A. Milanes,[62] M.-N. Minard,[4] D. S. Mitzel,[11] J. Molina Rodriguez,[60] I. A. Monroy,[62] S. Monteil,[5] M. Morandin,[22] P. Morawski,[27] A. Mordà,[6] M. J. Morello,[23,i] J. Moron,[27] A. B. Morris,[50] R. Mountain,[59] F. Muheim,[50] D. Müller,[54] J. Müller,[9] K. Müller,[40] V. Müller,[9] M. Mussini,[14] B. Muster,[39] P. Naik,[46] T. Nakada,[39] R. Nandakumar,[49] A. Nandi,[55] I. Nasteva,[2] M. Needham,[50] N. Neri,[21] S. Neubert,[11] N. Neufeld,[38] M. Neuner,[11] A. D. Nguyen,[39] T. D. Nguyen,[39] C. Nguyen-Mau,[39,n] V. Niess,[5] R. Niet,[9] N. Nikitin,[32] T. Nikodem,[11] D. Ninci,[23] A. Novoselov,[35] D. P. O'Hanlon,[48] A. Oblakowska-Mucha,[27] V. Obraztsov,[35] S. Ogilvy,[51] O. Okhrimenko,[44] R. Oldeman,[15,j] C. J. G. Onderwater,[67] B. Osorio Rodrigues,[1] J. M. Otalora Goicochea,[2] A. Otto,[38] P. Owen,[53] A. Oyanguren,[66] A. Palano,[13,o] F. Palombo,[21,p] M. Palutan,[18] J. Panman,[38] A. Papanestis,[49] M. Pappagallo,[51] L. L. Pappalardo,[16,a] C. Pappenheimer,[57] C. Parkes,[54] G. Passaleva,[17] G. D. Patel,[52] M. Patel,[53] C. Patrignani,[19,h] A. Pearce,[54,49] A. Pellegrino,[41] G. Penso,[25,q] M. Pepe Altarelli,[38] S. Perazzini,[14,f] P. Perret,[5] L. Pescatore,[45] K. Petridis,[46] A. Petrolini,[19,h] M. Petruzzo,[21] E. Picatoste Olloqui,[36] B. Pietrzyk,[4] T. Pilař,[48] D. Pinci,[25] A. Pistone,[19] A. Piucci,[11] S. Playfer,[50] M. Plo Casasus,[37] T. Poikela,[38] F. Polci,[8] A. Poluektov,[48,34] I. Polyakov,[31] E. Polycarpo,[2] A. Popov,[35] D. Popov,[10,38] B. Popovici,[29] C. Potterat,[2] E. Price,[46] J. D. Price,[52] J. Prisciandaro,[37] A. Pritchard,[52] C. Prouve,[46] V. Pugatch,[44] A. Puig Navarro,[39] G. Punzi,[23,r] W. Qian,[4] R. Quagliani,[7,46] B. Rachwal,[26] J. H. Rademacker,[46] M. Rama,[23] M. S. Rangel,[2] I. Raniuk,[43] N. Rauschmayr,[38] G. Raven,[42] F. Redi,[53] S. Reichert,[54] M. M. Reid,[48] A. C. dos Reis,[1] S. Ricciardi,[49] S. Richards,[46] M. Rihl,[38] K. Rinnert,[52] V. Rives Molina,[36] P. Robbe,[7,38] A. B. Rodrigues,[1] E. Rodrigues,[54] J. A. Rodriguez Lopez,[62] P. Rodriguez Perez,[54] S. Roiser,[38] V. Romanovsky,[35] A. Romero Vidal,[37] J. W. Ronayne,[12] M. Rotondo,[22] J. Rouvinet,[39] T. Ruf,[38] P. Ruiz Valls,[66] J. J. Saborido Silva,[37] N. Sagidova,[30] P. Sail,[51] B. Saitta,[15,j] V. Salustino Guimaraes,[2] C. Sanchez Mayordomo,[66] B. Sanmartin Sedes,[37] R. Santacesaria,[25] C. Santamarina Rios,[37] M. Santimaria,[18] E. Santovetti,[24,g] A. Sarti,[18,q] C. Satriano,[25,b] A. Satta,[24] D. M. Saunders,[46] D. Savrina,[31,32] M. Schiller,[38] H. Schindler,[38] M. Schlupp,[9] M. Schmelling,[10] T. Schmelzer,[9] B. Schmidt,[38] O. Schneider,[39] A. Schopper,[38] M. Schubiger,[39] M.-H. Schune,[7] R. Schwemmer,[38] B. Sciascia,[18] A. Sciubba,[25,q] A. Semennikov,[31] N. Serra,[40] J. Serrano,[6] L. Sestini,[22] P. Seyfert,[20] M. Shapkin,[35] I. Shapoval,[16,43,a] Y. Shcheglov,[30] T. Shears,[52] L. Shekhtman,[34] V. Shevchenko,[64] A. Shires,[9] B. G. Siddi,[16] R. Silva Coutinho,[48,40] L. Silva de Oliveira,[2] G. Simi,[22] M. Sirendi,[47] N. Skidmore,[46] I. Skillicorn,[51] T. Skwarnicki,[59] E. Smith,[55,49] E. Smith,[53] I. T. Smith,[50] J. Smith,[47] M. Smith,[54] H. Snoek,[41] M. D. Sokoloff,[57,38] F. J. P. Soler,[51] F. Soomro,[39] D. Souza,[46] B. Souza De Paula,[2] B. Spaan,[9] P. Spradlin,[51] S. Sridharan,[38] F. Stagni,[38] M. Stahl,[11] S. Stahl,[38] S. Stefkova,[53] O. Steinkamp,[40] O. Stenyakin,[35] S. Stevenson,[55] S. Stoica,[29] S. Stone,[59] B. Storaci,[40] S. Stracka,[23,i] M. Straticiuc,[29] U. Straumann,[40] L. Sun,[57] W. Sutcliffe,[53] K. Swientek,[27] S. Swientek,[9] V. Syropoulos,[42] M. Szczekowski,[28] T. Szumlak,[27] S. T'Jampens,[4] A. Tayduganov,[6] T. Tekampe,[9] M. Teklishyn,[7] G. Tellarini,[16,a] F. Teubert,[38] C. Thomas,[55] E. Thomas,[38] J. van Tilburg,[41] V. Tisserand,[4] M. Tobin,[39] J. Todd,[57] S. Tolk,[42] L. Tomassetti,[16,a] D. Tonelli,[38] S. Topp-Joergensen,[55] N. Torr,[55] E. Tournefier,[4] S. Tourneur,[39] K. Trabelsi,[39] M. T. Tran,[39] M. Tresch,[40] A. Trisovic,[38] A. Tsaregorodtsev,[6] P. Tsopelas,[41] N. Tuning,[41,38] A. Ukleja,[28] A. Ustyuzhanin,[65,64] U. Uwer,[11] C. Vacca,[15,j] V. Vagnoni,[14] G. Valenti,[14] A. Vallier,[7] R. Vazquez Gomez,[18] P. Vazquez Regueiro,[37] C. Vázquez Sierra,[37] S. Vecchi,[16] J. J. Velthuis,[46] M. Veltri,[17,s] G. Veneziano,[39] M. Vesterinen,[11] B. Viaud,[7] D. Vieira,[2] M. Vieites Diaz,[37] X. Vilasis-Cardona,[36,e] A. Vollhardt,[40] D. Volyanskyy,[10] D. Voong,[46] A. Vorobyev,[30] V. Vorobyev,[34] C. Voß,[63] J. A. de Vries,[41] R. Waldi,[63] C. Wallace,[48] R. Wallace,[12] J. Walsh,[23] S. Wandernoth,[11] J. Wang,[59] D. R. Ward,[47] N. K. Watson,[45] D. Websdale,[53] A. Weiden,[40] M. Whitehead,[48] G. Wilkinson,[55,38] M. Wilkinson,[59] M. Williams,[38] M. P. Williams,[45] M. Williams,[56] T. Williams,[45] F. F. Wilson,[49] J. Wimberley,[58] J. Wishahi,[9] W. Wislicki,[28] M. Witek,[26] G. Wormser,[7] S. A. Wotton,[47] S. Wright,[47] K. Wyllie,[38] Y. Xie,[61] Z. Xu,[39] Z. Yang,[3] J. Yu,[61] X. Yuan,[34] O. Yushchenko,[35] M. Zangoli,[14] M. Zavertyaev,[10,t] L. Zhang,[3] Y. Zhang,[3] A. Zhelezov,[11] A. Zhokhov,[31] L. Zhong,[3] and S. Zucchelli[14]

(LHCb Collaboration)

[1]*Centro Brasileiro de Pesquisas Físicas (CBPF), Rio de Janeiro, Brazil*
[2]*Universidade Federal do Rio de Janeiro (UFRJ), Rio de Janeiro, Brazil*
[3]*Center for High Energy Physics, Tsinghua University, Beijing, China*
[4]*LAPP, Université Savoie Mont-Blanc, CNRS/IN2P3, Annecy-Le-Vieux, France*
[5]*Clermont Université, Université Blaise Pascal, CNRS/IN2P3, LPC, Clermont-Ferrand, France*
[6]*CPPM, Aix-Marseille Université, CNRS/IN2P3, Marseille, France*

[7]LAL, Université Paris-Sud, CNRS/IN2P3, Orsay, France
[8]LPNHE, Université Pierre et Marie Curie, Université Paris Diderot, CNRS/IN2P3, Paris, France
[9]Fakultät Physik, Technische Universität Dortmund, Dortmund, Germany
[10]Max-Planck-Institut für Kernphysik (MPIK), Heidelberg, Germany
[11]Physikalisches Institut, Ruprecht-Karls-Universität Heidelberg, Heidelberg, Germany
[12]School of Physics, University College Dublin, Dublin, Ireland
[13]Sezione INFN di Bari, Bari, Italy
[14]Sezione INFN di Bologna, Bologna, Italy
[15]Sezione INFN di Cagliari, Cagliari, Italy
[16]Sezione INFN di Ferrara, Ferrara, Italy
[17]Sezione INFN di Firenze, Firenze, Italy
[18]Laboratori Nazionali dell'INFN di Frascati, Frascati, Italy
[19]Sezione INFN di Genova, Genova, Italy
[20]Sezione INFN di Milano Bicocca, Milano, Italy
[21]Sezione INFN di Milano, Milano, Italy
[22]Sezione INFN di Padova, Padova, Italy
[23]Sezione INFN di Pisa, Pisa, Italy
[24]Sezione INFN di Roma Tor Vergata, Roma, Italy
[25]Sezione INFN di Roma La Sapienza, Roma, Italy
[26]Henryk Niewodniczanski Institute of Nuclear Physics Polish Academy of Sciences, Kraków, Poland
[27]AGH - University of Science and Technology, Faculty of Physics and Applied Computer Science, Kraków, Poland
[28]National Center for Nuclear Research (NCBJ), Warsaw, Poland
[29]Horia Hulubei National Institute of Physics and Nuclear Engineering, Bucharest-Magurele, Romania
[30]Petersburg Nuclear Physics Institute (PNPI), Gatchina, Russia
[31]Institute of Theoretical and Experimental Physics (ITEP), Moscow, Russia
[32]Institute of Nuclear Physics, Moscow State University (SINP MSU), Moscow, Russia
[33]Institute for Nuclear Research of the Russian Academy of Sciences (INR RAN), Moscow, Russia
[34]Budker Institute of Nuclear Physics (SB RAS) and Novosibirsk State University, Novosibirsk, Russia
[35]Institute for High Energy Physics (IHEP), Protvino, Russia
[36]Universitat de Barcelona, Barcelona, Spain
[37]Universidad de Santiago de Compostela, Santiago de Compostela, Spain
[38]European Organization for Nuclear Research (CERN), Geneva, Switzerland
[39]Ecole Polytechnique Fédérale de Lausanne (EPFL), Lausanne, Switzerland
[40]Physik-Institut, Universität Zürich, Zürich, Switzerland
[41]Nikhef National Institute for Subatomic Physics, Amsterdam, The Netherlands
[42]Nikhef National Institute for Subatomic Physics and VU University Amsterdam, Amsterdam, The Netherlands
[43]NSC Kharkiv Institute of Physics and Technology (NSC KIPT), Kharkiv, Ukraine
[44]Institute for Nuclear Research of the National Academy of Sciences (KINR), Kyiv, Ukraine
[45]University of Birmingham, Birmingham, United Kingdom
[46]H.H. Wills Physics Laboratory, University of Bristol, Bristol, United Kingdom
[47]Cavendish Laboratory, University of Cambridge, Cambridge, United Kingdom
[48]Department of Physics, University of Warwick, Coventry, United Kingdom
[49]STFC Rutherford Appleton Laboratory, Didcot, United Kingdom
[50]School of Physics and Astronomy, University of Edinburgh, Edinburgh, United Kingdom
[51]School of Physics and Astronomy, University of Glasgow, Glasgow, United Kingdom
[52]Oliver Lodge Laboratory, University of Liverpool, Liverpool, United Kingdom
[53]Imperial College London, London, United Kingdom
[54]School of Physics and Astronomy, University of Manchester, Manchester, United Kingdom
[55]Department of Physics, University of Oxford, Oxford, United Kingdom
[56]Massachusetts Institute of Technology, Cambridge, Massachusetts 02139, USA
[57]University of Cincinnati, Cincinnati, Ohio 45221, USA
[58]University of Maryland, College Park, Maryland 20742, USA
[59]Syracuse University, Syracuse, New York 13244, USA
[60]Pontifícia Universidade Católica do Rio de Janeiro (PUC-Rio), Rio de Janeiro, Brazil (associated with Institution Universidade Federal do Rio de Janeiro (UFRJ), Rio de Janeiro, Brazil)
[61]Institute of Particle Physics, Central China Normal University, Wuhan, Hubei, China (associated with Institution Center for High Energy Physics, Tsinghua University, Beijing, China)
[62]Departamento de Fisica, Universidad Nacional de Colombia, Bogota, Colombia (associated with LPNHE, Université Pierre et Marie Curie, Université Paris Diderot, CNRS/IN2P3, Paris, France)

[63]*Institut für Physik, Universität Rostock, Rostock, Germany (associated with Physikalisches Institut, Ruprecht-Karls-Universität Heidelberg, Heidelberg, Germany)*
[64]*National Research Centre Kurchatov Institute, Moscow, Russia (associated with Institute of Theoretical and Experimental Physics (ITEP), Moscow, Russia)*
[65]*Yandex School of Data Analysis, Moscow, Russia (associated with Institution Institute of Theoretical and Experimental Physics (ITEP), Moscow, Russia)*
[66]*Instituto de Fisica Corpuscular (IFIC), Universitat de Valencia-CSIC, Valencia, Spain (associated with Institution Universitat de Barcelona, Barcelona, Spain)*
[67]*Van Swinderen Institute, University of Groningen, Groningen, The Netherlands (associated with Institution Nikhef National Institute for Subatomic Physics, Amsterdam, The Netherlands)*

[a]Also at Università di Ferrara, Ferrara, Italy.
[b]Also at Università della Basilicata, Potenza, Italy.
[c]Also at Università di Modena e Reggio Emilia, Modena, Italy.
[d]Also at Università di Milano Bicocca, Milano, Italy.
[e]Also at LIFAELS, La Salle, Universitat Ramon Llull, Barcelona, Spain.
[f]Also at Università di Bologna, Bologna, Italy.
[g]Also at Università di Roma Tor Vergata, Roma, Italy.
[h]Also at Università di Genova, Genova, Italy.
[i]Also at Scuola Normale Superiore, Pisa, Italy.
[j]Also at Università di Cagliari, Cagliari, Italy.
[k]Also at Universidade Federal do Triângulo Mineiro (UFTM), Uberaba-MG, Brazil.
[l]Also at AGH - University of Science and Technology, Faculty of Computer Science, Electronics and Telecommunications, Kraków, Poland.
[m]Also at Università di Padova, Padova, Italy.
[n]Also at Hanoi University of Science, Hanoi, Viet Nam.
[o]Also at Università di Bari, Bari, Italy.
[p]Also at Università degli Studi di Milano, Milano, Italy.
[q]Also at Università di Roma La Sapienza, Roma, Italy.
[r]Also at Università di Pisa, Pisa, Italy.
[s]Also at Università di Urbino, Urbino, Italy.
[t]Also at P.N. Lebedev Physical Institute, Russian Academy of Science (LPI RAS), Moscow, Russia.